Tenth U.S. National Conference on Earthquake Engineering
Frontiers of Earthquake Engineering
July 21-25, 2014
Anchorage, Alaska

UNCOVERING THE HETEROGENEITY OF SPATIAL LIFELINE SYSTEM INTERDEPENDENCIES

R. Paredes-Toro[1]*, L. Dueñas-Osorio[2], G. P. Cimellaro[3]

ABSTRACT

This paper performs a systematic exploration of spatial interdependencies across multiple lifeline networks; including power, water, fixed telephone and internet system, as representatives of modern smart infrastructure. The analysis expands a Kriging Aided Spatial Correlation Algorithm (KASCA) at the local scale and provides a more explicit and methodical formulation of the spatial approach. This is achieved by performing sensitivity analyses to best estimate the interdependence strengths across networks subjected to earthquakes across geographies that match predictions to field observations and local field features. The improved spatial analysis process is applied to the 2010 Mw 8.8 Chile Earthquake utility restoration data sets and the results are compared with previous temporal and spatial analyses for subsets of the systems. Results are communicated via local correlation maps and synthesized into global correlation plots, which can point out interdependence directionality and length of coupling influence. Addressing the spatial coupling behavior between networks is a crucial step towards achieving a univocal and robust quantification method of the interdependencies between lifeline systems and associated facilities**,** while also supporting predictive modeling and decision-making.

[1]Graduate Student, Dept. of Structural, Building & Geotechnical Engineering, Politecnico di Torino, Turin, ITALY.
[*]Research Intern, Dept. of Civil and Environmental Engineering, Rice University, Houston, TX 77251.
[2]Associate Professor, Dept. of Civil and Environmental Engineering, Rice University, Houston, TX 77251
[3]Assistant Professor, Dept. of Structural, Building & Geotechnical Engineering, Politecnico di Torino, Turin, ITALY.

Paredes-Toro R, Dueñas-Osorio L, Cimellaro G P. Uncovering the Heterogeneity of Spatial Lifeline System Interdependencies. *Proceedings of the 10th National Conference in Earthquake Engineering*, Earthquake Engineering Research Institute, Anchorage, AK, 2014.

Tenth U.S. National Conference on Earthquake Engineering
Frontiers of Earthquake Engineering
July 21-25, 2014
Anchorage, Alaska

Uncovering the Heterogeneity of Spatial Lifeline System Interdependencies

R. Paredes-Toro[1*], L. Dueñas-Osorio[2], G.P. Cimellaro[3]

ABSTRACT

This paper performs a systematic exploration of spatial interdependencies across multiple lifeline networks; including power, water, fixed telephone and internet system, as representatives of modern smart infrastructure. The analysis expands a Kriging Aided Spatial Correlation Algorithm (KASCA) at the local scale and provides a more explicit and methodical formulation of the spatial approach. This is achieved by performing sensitivity analyses to best estimate the interdependence strengths across networks subjected to earthquakes across geographies that match predictions to field observations and local field features. The improved spatial analysis process is applied to the 2010 Mw 8.8 Chile Earthquake utility restoration data sets and the results are compared with previous temporal and spatial analyses for subsets of the systems. Results are communicated via local correlation maps and synthesized into global correlation plots, which can point out interdependence directionality and length of coupling influence. Addressing the spatial coupling behavior between networks is a crucial step towards achieving a univocal and robust quantification method of the interdependencies between lifeline systems and associated facilities, while also supporting predictive modeling and decision-making.

Introduction

Various lifeline system models, either individually or coupled, have integrated post-event data and compared their predictions from numerical simulation and theoretical models with field-reported network responses after model calibration. The Graphical Iterative Response Analysis of Flow Following Earthquakes (GIRAFFE), a model that performs hydraulic analysis on water networks subjected to seismic damage, have been calibrated to the 1994 Northridge earthquake [1]. More recently, a calibration of the Interdependence Fragility Algorithm (IFA), a general-purpose seismic interdependence damage propagation model [2], to data obtained from the 2010 Chile earthquake was performed [3]. However, authors of these and related studies note that additional refinements to network component fragility estimation and interdependence strength quantification are needed to further improve network vulnerability predictions, particularly for systems that include buried networks like water and gas, and systems with not well understood coupling interfaces across them.

[1] Graduate Student, Dept. of Structural, Building & Geotechnical Engineering, Politecnico di Torino, Turin, ITALY.
[*] Research Intern, Dept. of Civil and Environmental Engineering, Rice University, Houston, TX 77251.
[2] Associate Professor, Dept. of Civil and Environmental Engineering, Rice University, Houston, TX 77251
[3] Assistant Professor, Dept. of Structural, Building & Geotechnical Engineering, Politecnico di Torino, Turin, ITALY.

Paredes-Toro R, Dueñas-Osorio L, Cimellaro G P. Uncovering the Heterogeneity of Spatial Lifeline System Interdependencies. *Proceedings of the 10th National Conference in Earthquake Engineering*, Earthquake Engineering Research Institute, Anchorage, AK, 2014.

In fact, when assessing multi-network component fragility, an important factor to take into account, besides the fragility of components, is the *interdependence strength* between infrastructure system facilities. A time series approach [4] applied to restoration curves of infrastructures after the 2010 Chile earthquake was capable of estimating the interdependent coupling strengths between diverse networks and relate them to overall component and system-level functionality; also, other authors have adopted this methodology in different seismic events [5]. However, interdependence strength is variable across geographies, and thus a spatial focus to infrastructure systems is warranted besides their temporal aggregated effects. For instance, the Kriging Aided Spatial Correlation Algorithm (KASCA) [6]; is a methodology that analyzes the cross-correlation between network restoration patterns considering their actual spatial distribution. This approach provides insights on how multiple coupling locations and local features of the built environment affect interdependence, how influential coupling effects are as a function of distance, and how directionality effects could emerge from the multi-utility restoration patterns in space.

This paper performs a systematic exploration of spatial restoration processes on several coupled modern lifeline networks using restoration post-event data, and contributes to model development and sensitivity analyses from the application of ordinary point kriging to estimate interdependence strengths of networks subjected to earthquakes. This spatial-based methodology is expanded at the local scale and applied to four lifeline networks, which were particularly affected by the 2010 Mw 8.8 Chile Earthquake. Results are then analyzed relative to field data and local features, as well as qualitatively compared to previous analyses involving related networks and metrics. Kriging surfaces have been implemented in few seismic hazard applications [7,8] for earthquake hazard zoning for areas of Indonesia and Mexico. However, KASCA is the only implementation on interdependence quantification efforts.

The remainder of this paper is structured as follows: Section 2 summarizes the mathematical concepts that underpin the proposed methodology for correlation coefficients derivation across networks via kriging surfaces. Section 3 discusses the application of these concepts and strategies to derive spatial correlations in the context of the 2010 Chile earthquake and four lifeline systems, including power, water, fixed telephones and internet. Section 4 discusses the results from the methodology presented in this paper as well as new insights of the spatial coupling analyses. Section 5 discusses the main conclusions from this study and directions for future research.

Mathematical Concepts for Spatial Correlation Analysis of Lifeline Interdependencies

Pearson's correlation coefficient has already been used as a measure of association to quantify the degree of interdependence between infrastructure systems [9]. Pearson's coefficient ρ [10] describes the degree of linear correlation between two sets of data, and it is a generally accepted metric [4, 11]. In this paper, ρ is used with the spatially distributed restoration potential data, denoted $\psi_{j,zi}$, with j taking the form of P, W, T and I referring to the Power, Water, Telephone and Internet systems, respectively, and Z indicating the point of evaluation in the horizontal plane. Hence, $\psi_{j,zi}$ values are spatially distributed points capturing restoration times, which are then used to derive correlations across points between networks. In the context of network analysis, spatial correlations of datasets from the same network (i.e. P→P) describe the auto-correlation, (which relate to intra-network dependency) while spatial correlations of datasets from different networks

describe their cross-correlation (i.e. P→W), which relate to inter-network dependency.

Before starting the spatial correlation analysis is necessary to construct kriging surfaces in $\psi_{j,zi}$ data to enable interpolation and interrogation of data values at particular spatial coordinates for interdependent correlation analysis. The kriging calculation first requires the formulation of a variogram, which describes the spatial dependency of observations in sets containing $\psi_{j,zi}$ points. The process of estimating the variogram from sampled data is called variography. It begins with the calculation of the variogram estimator derived from the raw data [12]:

$$\gamma_E(h) = \frac{1}{2N(h)} \sum_{i=1}^{N(h)} (\psi_{j,zi} - \psi_{j,zi+h})^2 \tag{1}$$

where $\psi_{j,zi}$ and $\psi_{j,zi+h}$ denote the restoration potential for a system j evaluated at points z_i and z_i+h and $N(h)$ describes the number of pairs of points within the lag interval h, taken to be the Euclidian distances between the two points i and $i+h$ and may be set equal to the mean minimum distance between pairs. The variogram model is a parametric curve fitted to the variogram estimator. Many models are available for this, including the spherical, exponential, and Gaussian models [13]; however, some considerations must be accounted for when fitting them to the variogram estimator. Some preliminary guidelines derived from sensitivity analyses are proposed. When using Eq. 1, considerations applied in geostatistics are a good starting point; nevertheless, caution must be taken in regards to the lag size h. The size of the lag interval must be small enough to capture the evolution of the variogram at local scales, where the most relevant semivariances for the kriging procedure are used. Additionally, when modelling the variogram, one should not consider the nugget effect, which is the intercept with the ordinate and has the potential to produce discontinuities on the kriging surface between sampled data and interpolated locations.

Ordinary point kriging interpolates the $\psi_{j,zi}$ values at a particular point z_P by calculating the weighted average of $\psi_{j,zi}$ values evaluated at an N number of neighboring points. This interpolation is expressed in Eq. 2, where λ_i is the weighting coefficient associated with point z_i that must be estimated satisfying the constraints in Eqs. 3 and 4, while minimizing the mean-squared error in Eq. 5.

$$\hat{\psi}_{j,z_P} = \sum_i^N \lambda_i \psi_{j,z_i} \tag{2}$$

$$\sum_i^N \lambda_i = 1 \tag{3}$$

$$E(\hat{\psi}_{j,z_P} - \psi_{j,z_P}) = 0 \tag{4}$$

$$E((\hat{\psi}_{j,z_P} - \psi_{j,z_P})^2) = 2\sum_{i=1}^N \lambda_i \gamma(z_i, z_P) - \sum_{i=1}^N \sum_{k=1}^N \lambda_i \lambda_k \gamma(z_i, z_k) \tag{5}$$

where $\psi_{j,zp}$ is the true but unknown value of ψ_j evaluated at a particular point z_P and $\gamma(z_i,z_k)$ is the variogram between values at zi and z_k. The optimization problem is solved using a Lagrange-multiplier v, resulting in a linear kriging system of $N+1$ equations. One equation is already

expressed in Eq. 3, and the i^{th} equation of the remaining N becomes [14]:

$$\sum_{k=1}^{N} \lambda_k \gamma(z_i, z_k) + \nu = \gamma(z_i, z_P) \tag{6}$$

A simple illustrative example for spatial interpolation with ordinary point kriging is developed next. Fig. 1 depicts a slice of a generic spatial stochastic process varying in a two dimensional space that has been sampled at points 1, 2, 3, 4 and 5. Assume that an estimate of the random variable describing the field values is needed at location P. One can solve this problem by applying the ordinary point kriging interpolation method.

The process starts with the variography. First, compute all pairwise empirical semi-variances (Fig. 1). Then, fixing the lag size h to 1 meter, use Eq. 1 to compute the variogram estimator at each interval. Fit a linear model to the averaged semi-variances deriving from the variogram estimator. Use the fitted model to compute the semi-variances needed in Eq. 6 and solve for all λ_i and ν, using Eq. 3 as well. Finally, using Eq. 2 we compute $Z_P = 101.75$. It should be noted that in this example a very reduced population was considered and a linear model was used; however, in applications, a greater population should be used and more complex models through weighted least-squares fitting can be adjusted [13].

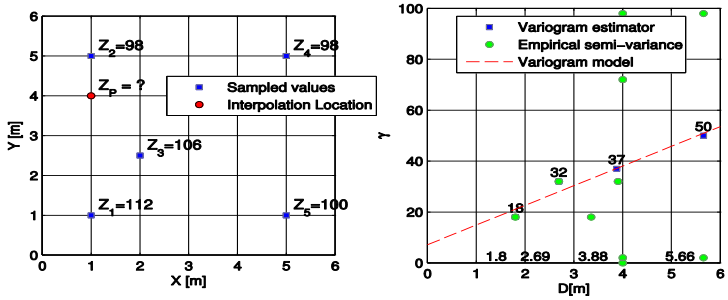

Figure 1. Left, sampled and desired estimate locations. Right, graphical representation of the experimental variogram, the variogram estimator and the variogram model.

The spatial correlation analysis strategy for infrastructure data adopted in this paper starts at the local scale defining a polar mesh around each evaluation node, referred to as the local mesh, where $\psi_{j,zi}$ is interpolated using the kriging concepts. Then, local sets of values $\psi_{j,zi}$ and $\psi_{k,zi}$. are correlated .Successively kriging the results over the defined meshes *local correlation maps* are constructed. These maps quantify geospatially the degree of association between restoration patterns. Starting again from the surfaces, we can also correlate all the set of $\psi_{j,zi}$ at the evaluation nodes with the interpolated $\psi_{j,zi}$ set shifted at a certain distance and direction in the local meshes. We represent the previous results in polar contour plots called *global correlation maps* and we use them to study the anisotropy of spatial correlation. Finally, we average the previous results in all directions to study the correlation range as function of distance, to quantify the *length of interdependence*. In general, if both sets are referring to the same network for the global analysis, intra-dependence coefficients are estimated; otherwise, the computed correlation coefficients depict inter-dependence between the respective networks.

Estimating Spatial Interdependence with Kriging Surfaces for Field Data

The kriging-based spatial correlation strategies are applied for the first time to the power, water, telephone and internet network systems of the Talcahuano-Concepción area of Chile, in the context of the 27 February 2010 M_W 8.8 Offshore Maule earthquake. The restoration potential takes the form of days of repair to service full restoration, which is the field collected post-event data at various locations (evaluation nodes). For the power and water networks N = 94, while for the telephone and internet networks N = 70.

Spatial correlation analyses require kriging surfaces to include values at additional coordinates (Z_i), describing various R Euclidian distances from each evaluation node at coordinates (Z_P), with varying θ angles in the horizontal plane. Thus, a mesh of (Z_i) coordinates is created using distance increments ΔR of 125 m up to a maximum distance R of 2.5 km and angle increments $\Delta\theta$ of $\pi/20$ in the horizontal plane. Kriging surfaces of $\psi_{j,zi}$ values are derived within this mesh for each network. The resulting kriging surfaces (Fig. 2) are presented as a cloud of points describing the value of $\psi_{j,z}$ at those points.

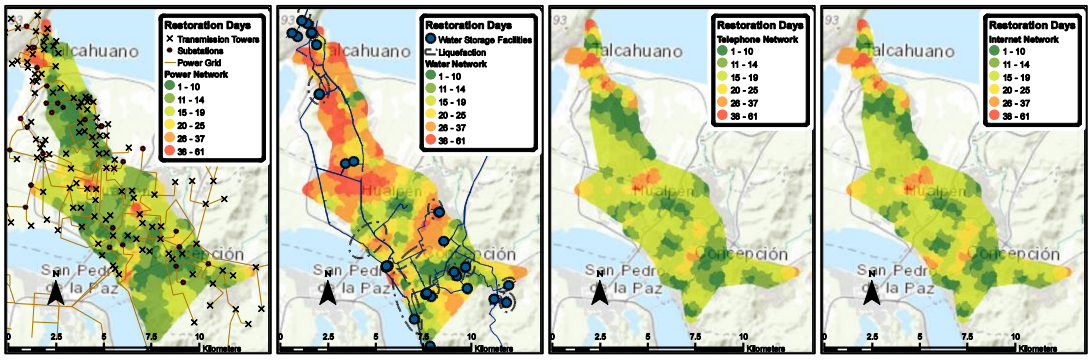

Figure 2. Kriging surfaces of the four lifeline systems considered. Restoration potential $\psi_{j,z}$ expressed in days of repair to service full restoration.

Computing the local correlation between the $\psi_{j,zi}$ values in a local mesh with the $\psi_{k,zi}$ values in the same mesh results into a correlation value located at the evaluation node. Repeating this process for all local meshes and successively kriging results leads to the local correlation maps in Fig. 3, which depict the rich heterogeneity in interdependence. Then, global correlation analysis is pursued to synthesize local trends. Consider set X as all evaluation nodes in network j and set Y as all interpolated nodes in network k, but shifted by a distance R_P and a direction θ_P from the center of the local meshes (an evaluation node). Then, we correlate the sets and locate that correlation coefficient in a polar grid with coordinates R_P and θ_P. By repeating this process, fixing set X as reference and varying set Y for all ΔR and $\Delta\theta$ increments from 0 to $2.5km$ and from 0 to 2π respectively, yields to a global correlation map between two networks (Figs. 4 and 5). Finally, averaging the previous results in the θ direction allows studying spatial correlation as a function of distance only. The error bars in Fig. 6 depict one standard deviation from the mean. All these results are studied next.

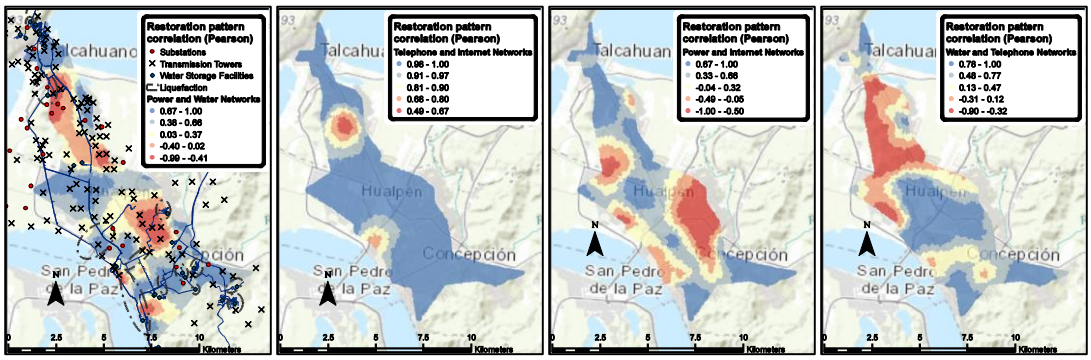

Figure 3. Local correlation maps between power and water (P→W), telephone and internet (T→I), power and internet (P→I) and water and telephone networks (W→T).

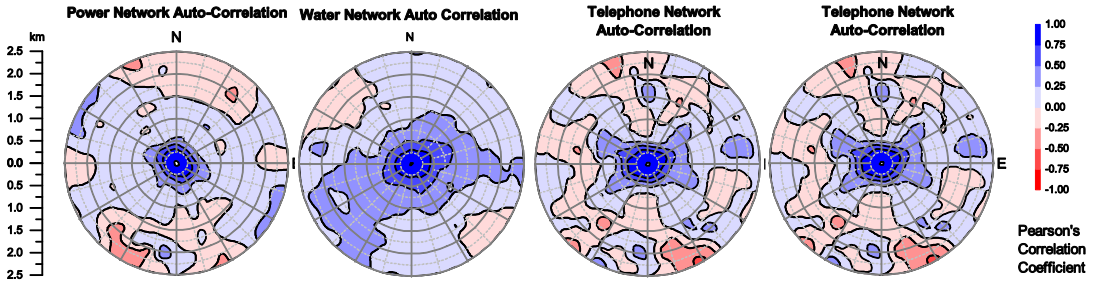

Figure 4. Global spatial autocorrelation maps of all lifeline networks.

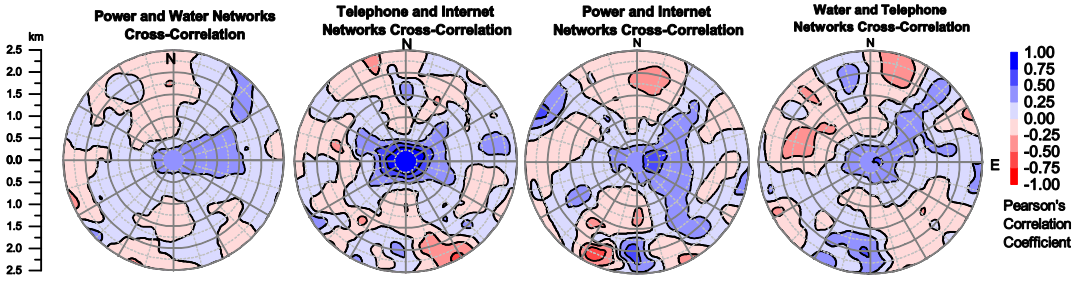

Figure 5. Global spatial cross-correlation maps between various lifeline networks.

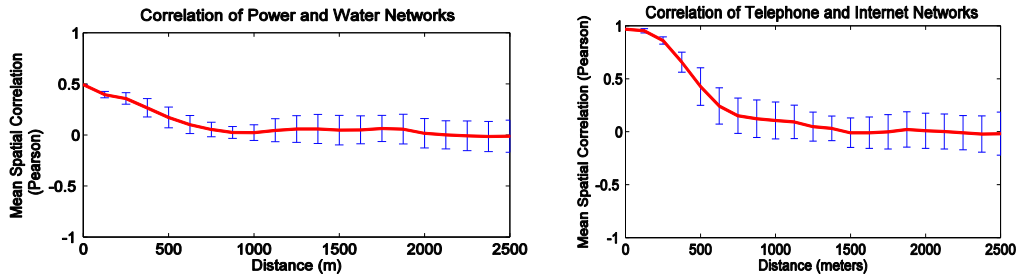

Figure 6. Left, average cross-correlation plots between the power and water network. Right, average correlation plots between the telecommunication networks.

Analysis of KASCA Results

The kriging surface in Fig. 2 representing the power network restoration shows that most of the recovering finished within 15 days after the event; peaks in the surface represent major delays matching the locations of electrical substations and transmission lines that could have been particularly affected by the earthquake. In addition, the water network restoration surface indicates that the recovering started at the south part of the studied area, where the water treatment plant intake is located, and continued towards the north; similarly, peaks out of the trend of the restoration scheme match zones in which liquefaction was verified. In relation to the recovering of the telephone and internet networks, both surfaces are quite similar supporting the fact that they share similar infrastructure; also, the surfaces seem to be delayed with respect to the power network restoration surface, confirming the great impact that the power outage had in the telecommunication network systems [15].

Local correlation maps in Fig. 3 capture the interdependent behavior of network pairs, such as the water and the power networks, where negative correlation is interpreted as distortion due to aggregate effects (i.e. liquefaction damaging pipelines). They also captured the simultaneous loss of connectivity between the telecommunication services and the central offices by presenting a uniform distribution of high correlation values across the region. The interaction between the power and internet network was not as uniform as expected, because of the damages in the specific components of the telecommunication and the power network. Local correlation maps depicted assistance from the telephone network to the water network restoration logistics.

The global correlation maps in Fig. 4 and 5, overall, present high correlation towards the center, while correlation generally decreases as the distance from the center increases. For the autocorrelation this value is exactly 1 at the center but when cross-correlations are computed the value at the center can be interpreted as the global coupling strength between networks sharing the same geospatial distribution. However, it can be observed that for all plots the correlations are not radially symmetric. Global auto-correlation maps for the water network (Fig. 4) demonstrate that towards the north and south, matching the geometry of the pipelines crossing Talcahuano and Concepción areas (Fig. 2), the correlation practically vanishes, but towards the east and west it does not vanishes completely. This suggest that the restoration of the water network facilities granted functionality to adjacent facilities towards the east and west from the pipelines but until the labors of restoration in the main pipelines are not progressing towards the north, northern facilities and users are not gaining functionality. Fig. 5 depicts favored coupling between the power and water systems towards the east, meaning that there is a large interdependent area in which water facilities are being supplied with electricity from service areas within distances reaching 1.5 kilometers. The global correlation map in Fig. 5 referring to the telecommunication networks indicates that the directionality was not as imperative as distance in the interdependence phenomenon. The restoration pattern of the power network aided the internet networks to recover towards the south-east (Fig. 4), indicating supplying of electricity at great distances and the absence of backup resources in the internet network in this direction. Finally, the global correlation map integrating the water and telephone networks depicts support from the telecommunication network in the repair efforts of the water network towards the north-east and west.

In relation to the correlation plots in Fig. 6, their correlation vanishes after approximately 1.5 kilometers. Regarding the different shapes of the curves, the telecommunication stays constant and then decreases suddenly after around 200 meters, while the power and water networks present a linear decreasing trend of the coupling behavior. This could be explained by the fact that the telecommunication networks do not operate in a fixed topology and its components are connected wirelessly within a certain range of coverage, once exceeded this range, the association of systems restoration involves more components performing diversely, decreasing the correlation estimates for small increments of distance. In contrast, the power and water network are constrained to their physical layout and present physical connections at closer distances that affect the correlation estimates progressively along the influence length. In addition, the telephone and internet networks presented the highest coupling strengths; this is explained after realizing that both networks are using digital technology, and then, both services could be connected to the same central offices in which their equipment was affected by the event.

Conclusions

This paper expanded the kriging aided spatial correlation algorithm (KASCA) [6], by introducing guidelines for the formulation of the kriging surfaces and deriving local correlation maps, global correlation maps and averaged correlation plots for a larger number of coupled lifeline systems. The enhanced approach was applied to power, water, telephone, and internet lifeline systems performing during the 2010 Mw 8.8 Chile Earthquake to capture interdependence strength, directionality and length.

The kriging surfaces resulting from this methodology provide a realistic estimate of lifelines performance by matching available actual responses. Also, local correlation maps are able to establish coupling strength estimates between networks and their components, and when not possible, they point out aggregated effects due to adopted repair schemes or liquefaction damages to buried networks. Global correlation maps verified directionality of the coupling behavior between networks for the water and power network and a less anisotropic behavior for the telecommunication networks. Averaged correlation plots provided estimates referring to the length of interdependence of around 1.5 kilometers and coupling strengths for all pairwise networks of 0.494, 0.554 , 0.502, 0.504, 0.471 and 0.969 (P→W, P→T, P→I, W→T, W→I and T→I, respectively). These correlation values compare dequately to results obtained in similar analyses for the same water and power networks aggregated at regional and city levels [4].

The applied methodology provides simulation models that yield realistic coupling strengths and influence lengths considering the relative position of network facilities. When using real time data this method can aid the decision making. For instance, global autocorrelation maps can identify directions in which restoration efforts are not having impact in the overall restoration of a network or directions in which the level of damage was more severe to identify broken connections or change direction of repair scheme to optimize restoration. Global crosscorrelation maps can indicate until which spatial extent restoring a network is assisting other network so extra resources can be allocated as needed. Global autocorrelation and crosscorrelation plots provide a length of correlation that can help selecting the size of the backup, crews and material resources.

Future research should aim to integrate the state of restoration at varying points in time, as found in time series correlation approaches [4], but for every point in space for a joint spatial-temporal description of interdependence. This would particularize the correlation estimates towards the specific component level of detail, quantifying for each of them the interdependence among components pertaining or not to the same network, their directionality and length of influence.

Acknowledgments

The present work has been funded in part by the National Science Foundation through grant CMMI-0748231. This support is gratefully acknowledged. Any opinions, findings and conclusions or recommendations expressed in this work are those of the authors and do not necessarily reflect the views of the National Science Foundation. The authors also would like to thank Dr. Mauricio Villagrán, his support with data collection and technical discussions; and finally to Jason Wu for starting the development of KASCA.

References

[1] Bonneau, A. and O'Rourke, T.D. Water Supply Performance during Earthquakes and Extreme Events. MCEER, University at Buffalo. Buffalo, New York, 2009.

[2] Hernandez-Fajardo, I., and Dueñas-Osorio, L. Sequential Propagation of Seismic Fragility across Interdependent Lifeline Systems. Earthquake Spectra. 2011: 27, 23-43.

[3] Wu J, Dueñas-Osorio L. Calibration and Validation of a Seismic Damage Propagation Model for Interdependent Infrastructure Systems. *Earthquake Spectra*. 2013; 29(3):1021–1041.

[4] Dueñas-Osorio L, Kwasinski A. Quantification of Lifeline System Interdependencies after the 27 February 2010 M_w 8.8 Offshore Maule, Chile, Earthquake. *Earthquake Spectra*. 2012. 28, 581-603.

[5] Cimellaro GP, Asce AM, Solari D, Renschler CS, Reinhorn AM. Community resilience index integrating network interdependencies. *Structures Congress.* 2013: 1789-1799.

[6] Wu J, Dueñas-Osorio L. Spatial Quantification of Lifeline System Interdependencies. *Proceedings of the 15th World Conference on Earthquake Engineering*. Lisbon, Portugal, 2012.

[7] Irwansyah E, Winarko E, Rasjid ZE, Bekti RD. Earthquake hazard zonation using peak ground acceleration (PGA) approach. *Journal of Physics: Conference. Series*. 2013.423; 012-067.

[8] Osorio L, Mayoral JM. Seismic microzonation for the northeast Texcoco lake area, Mexico. *Soil Dynamics and Earthquake Engineering*. 2013;48: 252–266.

[9] Mendonça D, Wallace WA. Impacts of the 2001 World Trade Center Attack on New York City Critical Infrastructures. *Journal of Infrastructure Systems*. 2006:12,260–270.

[10] Rodgers J., Nicewander W. Thirteen Ways to Look at the Correlation Coefficient. The American Statistician 1988;42:59 – 66.

[11] Kendall, M. and Gibbons, J.D. Rank Correlation Methods. *5th ed. Oxford University Press*. New York, 1990.

[12] Matheron G. *Les Variables Régionalisées et leur Estimation*. Masson. Paris, 1965.

[13] Oliver M., Webster R. A tutorial guide to geostatistics, computing and modelling variograms and kriging. *Catena.* 2014;113:56–69.

[14] Trauth M. *Matlab Recipes for Earth Sciences*. Springer. Meppel, 2007.

[15] Technical Council on Lifeline Earthquake Engineering. *Chile Earthquake of 2010: Lifeline Performance*. Monograph Series N° 36. United States of America. 2013: